*Energies* **2015**, *8*, 11515-11530; doi:10.3390/en81011515

OPEN ACCESS

*energies*

**ISSN 1996-1073**

www.mdpi.com/journal/energies

*Article*

# Optimal Tilt Angle of Photovoltaic Arrays and Economic Allocation of Energy Storage System on Large Oil Tanker Ship

**Hai Lan [1], Jinfeng Dai [1], Shuli Wen [1,*], Ying-Yi Hong [2], David C. Yu [3] and Yifei Bai [1]**

[1] College of Automation, Harbin Engineering University, Harbin 150001, Heilongjiang, China; E-Mails: lanhai@hrbeu.edu.cn (H.L.); daijinfeng@hrbeu.edu.cn (J.D.); baiyifei@hrbeu.edu.cn (Y.B.)

[2] Department of Electrical Engineering, Chung Yuan Christian University, Chung Li 32023, Taiwan; E-Mail: yyhong@dec.ee.cycu.edu.tw

[3] Department of Electrical Engineering and Computer Science, University of Wisconsin-Milwaukee, Milwaukee, WI 53211, USA; E-Mail: yu@uwm.edu

* Author to whom correspondence should be addressed; E-Mail: wenshuli@hrbeu.edu.cn; Tel./Fax: +86-451-8256-8560.

Academic Editor: Tapas Mallick

*Received: 21 August 2015 / Accepted: 9 October 2015 / Published: 15 October 2015*

**Abstract:** This study optimizes the tilt angle of photovoltaic (PV) panels on a large oil tanker ship system and considers the impact of partial shading to improve the performance of the PV system. This work presents a novel method that considers the difference between the expected and real outputs of PV modules to optimize the size of energy storage system (ESS). The method also takes into account the cost of wasted power, the capital cost of the system, fuel cost and the $CO_2$ emissions. Unlike on land, power generation using a PV on a ship depends on the date, latitude and longitude of the navigation. Accordingly, this work considers a route from Dalian in China to Aden in Yemen, accounting for the seasonal and geographical variations of solar irradiation. This proposed method adopts five conditions associated with the navigation route to model the total shipload. Various cases are discussed in detail to demonstrate the effectiveness of the proposed algorithm.

**Keywords:** tilt angle; photovoltaic (PV) panels; oil tanker ship system; energy storage system (ESS); $CO_2$ emissions

## 1. Introduction

Owing to strict restrictions that have been imposed by the International Convention for the Prevention of Pollution from Ships (MARPOL) [1] and the rapid development of renewable energy, solar power generation and energy storage systems (ESSs) on ships have been increasingly attracting attention. In a traditional ship power system, power is supplied only by a diesel generator, which causes serious environmental pollution and has low energy efficiency [2]. According to the previous investigations [3–6], the integration of solar energy and ESSs is one of the best solutions to reduce greenhouse gas emissions, improve energy efficiency and improve the stability of a ship's power system.

However, the improper installation of photovoltaic (PV) arrays increases the cost of power and its loss, especially on ships. In recent years, several studies have been performed to optimize the tilt angle of PV panels [7–12]. Karakose and Baygin [13] presented a method for optimizing the location of PV modules under consideration of different shaded working conditions. Sharma *et al.* [14] proposed a comprehensive parametric model of a flexible PV array, in support of its economic operation under dynamic and extreme environmental conditions. Their model considered the impact of various non-uniform environmental conditions and tilt angles to maximize power extraction. Midtgard *et al.* [15] presented a theoretical model that optimizes the design of the PV array and they analyzed the efficiencies of PV modules under various conditions. Shirzadi *et al.* [16] developed a novel approach for finding the optimal arrangement of modules in an array that minimizes mismatch losses more effectively than conventional methods. Due to the serious partial shading influence on the power generation of PV arrays, Díaz-Dorado *et al.* [17] utilized a metaheuristic method that is based on evolution strategies to calculate the best tilt angles of PV panels, considering the shading effect of obstacles and PV trackers. Indu Rani *et al.* [18] enhanced power generation from PV modules under partial shading conditions using Su-Do-Ku Configuration approach. Paraskevadaki and Papathanassiou [19] optimized the output power of PV arrays considering shadow effect.

The integration of a significant amount of PV power into a ship power system to reduce $CO_2$ emission is challenging so ESSs play a critical role in ensuring the stability of the hybrid ship system and the quality of the power output. Studies [20–23] have found that the use of an ESS is one of the most effective ways to ensure the reliability and power quality of power systems and favors the increased penetration of distributed generation resources. Some investigations [24–26] have demonstrated that the optimal management of ESS with distributed generators in power systems can reduce the cost and loss of power; improve the voltage profile; shave the peak load; and reduce the negative impact of power generation on the environment.

A ship power system with PV and ESS can be regarded as a special mobile and islanded microgrid. However, to the best of the authors' knowledge, the hybrid PV/diesel/battery ship power system has not been widely discussed. Ovrum and Bergh [27] explored various strategies of controlling battery for operating a ship crane. The use of battery storage systems to convert bulk carriers to all-electric ships for maximizing fuel savings has also been examined [28].

This paper presents an optimization analysis for the installation of PV panels in a hybrid ship power system that is used in a real oil tanker ship of 100,000 dwt (deadweight), integrating PV modules and ESS, taking the shading factor into consideration. A novel method that exploits the difference between the expected and real output power of a PV system is proposed to optimize the size of the ESS in a standalone ship's power system for use on a typical navigation route from Dalian in China to Aden in Yemen. Specifically, the generated power from PV arrays on the shipboard is corrected by the proposed method to account for the influence on the change in position of the ship along that route. Variations of the load under five conditions are modeled; these conditions are regular cruising, full-speed sailing, docking, loading/unloading and anchoring. For the economic analysis, the Multi-Objective Genetic Algorithm (MOGA) is used to determine the optimal sizes of various sources of power and to minimize $CO_2$ emissions.

The rest of this paper is organized as follows. Section 2 models the hybrid ship power system. Section 3 formulates the problem. Section 4 presents the solution method. Section 5 describes different case studies to validate the proposed algorithm and Section 6 draws conclusions.

## 2. Hybrid Ship Power System and Components

### *2.1. Problem Description*

Unlike generation systems on land, a ship's power system operates always in a mobile and islanded mode. When a ship sails, it receives continuously varying irradiation even though the solar radiation is fixed. Additionally, the total load varies with the operating conditions of the ship.

This study analyzes the optimal angle of installation of PV panels in a ship's power system, taking into account the environment along the navigation route. The cost and emissions of a hybrid PV/diesel/ESS power system in an oil tanker ship are optimized using a novel method based on the structure of the oil tanker, as presented in Figure 1. The system comprises a generating PV array, a diesel generator to supply the main power and an ESS to store excess energy and improve the reliability of the system. The diesel generator must be able to supply the whole load at all times since the ship's power system only operates in stand-alone mode. The dimensions of this oil tanker are 332.95 m long by 60 m wide by 30.5 m high. The available area for PV array installation is 2000 $m^2$.

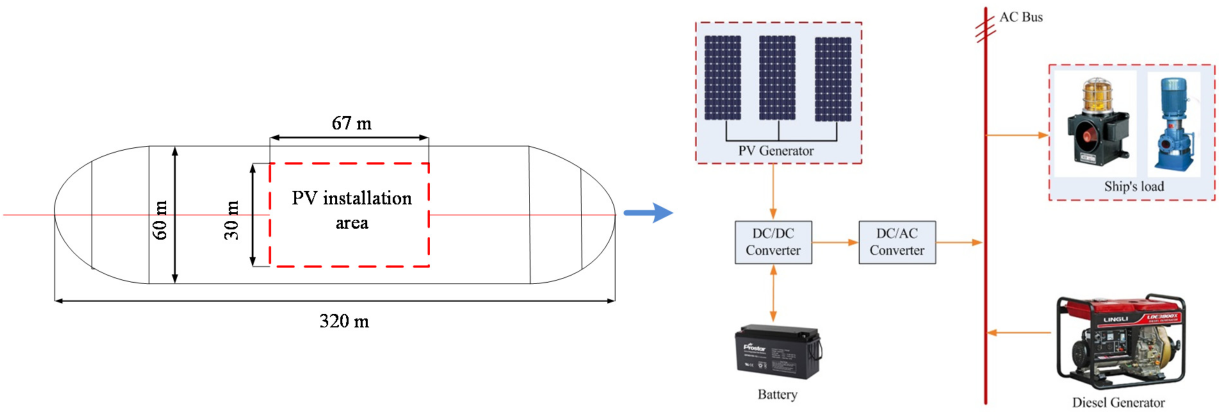


**Figure 1.** Hybrid ship power system.

The oil tanker takes 20 days to navigate from Dalian in China to Aden in Yemen and the navigation route is displayed in Figure 2. The oil tanker sails five times annually. Specifically, the ship sets sail at 8:00 a.m. on 4 January, 26 February, 20 April, 12 June, and 4 August from Dalian in China and returns on 28 January, 22 March, 14 May, 6 July, and 28 August from Aden in Yemen. Consequently, the optimization involves 4800 h in a year.


**Figure 2.** Navigation route of oil tanker.

## *2.2. Models of System Components*

### 2.2.1. PV System

Solar irradiation varies with the location of the ship, the date and the time, as the oil tanker sails along the route. Therefore, the power that is generated by the PV arrays on board must be calculated in a manner that takes into account the time, the longitude, and the latitude. This work establishes a mathematical model for estimating the power output of PV modules. The output power of the PV system at time $t$ ($t$ = 1, 2,…, 4800) is obtained from the solar radiation using following formula:

$$P_{\mathrm{PV}(t)} = \eta_{\mathrm{pv}} \times A_{\mathrm{pv}} \times I_{(t)} \quad (1)$$

where $\eta_{\mathrm{pv}}$ is the instantaneous PV generator efficiency; $A_{\mathrm{pv}}$ is the area of modules that are used in the PV system (m$^2$), and $I_{(t)}$ is the hourly total solar radiance (W/m$^2$).

Solar irradiation is crucial to a hybrid ship power system and the total solar irradiation comprises three parts that are the direct radiation, sky diffuse radiation, and the ground reflected radiation. This work proposes a modification of the hourly total solar radiance on board as follows:

$$I_{(t)} = I_{b(t)} + I_{d(t)} + I_{r(t)} = \left(I_{bh(t)} + \frac{I_{dh(t)} I_{bh(t)}}{I_{o(t)}}\right) R_b + \frac{I_{bh(t)}}{2I_{o(t)}}[I_{o(t)} - I_{bh(t)}](1+\cos\beta) + \frac{1}{2}\rho\,(I_{dh(t)} + I_{bh(t)})(1-\cos\beta) \quad (2)$$

where $I_{b(t)}$, $I_{d(t)}$, $I_{r(t)}$, $I_{bh(t)}$, $I_{dh(t)}$, and $I_{o(t)}$ denote the direct radiation, sky diffuse radiation, the ground reflected radiation, the direct radiation on horizontal surfaces, the diffuse radiation on horizontal surfaces, and the direct normal irradiance on a surface perpendicular to the sun's rays, respectively. Note that the different types of irradiation ($I_{b(t)}$, $I_{d(t)}$ and $I_{r(t)}$) are all influenced by the direct radiation on the horizontal surface ($I_{bh(t)}$). The variables ρ and β represent the albedo, which is taken to be 0.2 [29] in this paper, and the angle between the PV panel and the board, respectively. The variable $R_b$ is the ratio of the radiation that hits the tilt surface to that which hits the horizontal surface, which is given by Equation (3).

$$R_b = \frac{\cos(\phi - \beta)\cos\delta\cos\omega_s + \sin(\phi - \beta)\sin\delta}{\cos\phi\cos\delta\cos\omega_s + \sin\phi\sin\delta} \quad (3)$$

where $\phi$ is the local latitude; $\omega_s$ is solar hour angle (noon is zero, the morning is positive, the afternoon is negative), and $\delta$ represents the solar declination angle. Equations (4) and (5) yield the solar hour angle and the declination angle [30]:

$$\omega_s = \arccos(-\tan\phi \cdot \sin\delta) \quad (4)$$

$$\delta = 23.45 \ \sin[360 \times (284 + n) / 365] \quad (5)$$

where $n$ is the date with 1 January equal to one.

When the PV arrays are installed in a certain tilt angle, the shadow of the front arrays will have a large effect on the output of the arrays behind them. Specifically, the efficiency of PV modules decreases by approximately 20% if ignoring the shading factor [31]. This paper analyzes the optimal tilt angel for PV installation on shipboard under consideration of shading influence, which is shown in Figure 3. Assume that the reverse-biased diode is utilized in PV arrays herein and MPPT is still working while partial shading occurs.

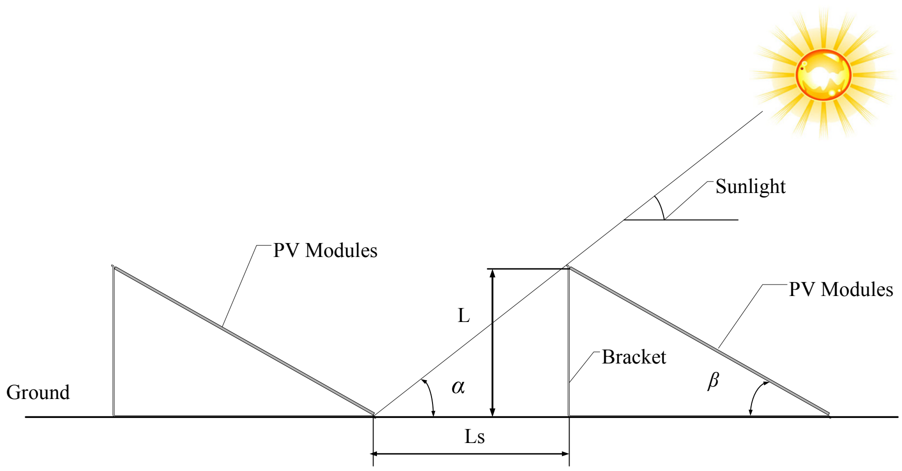


**Figure 3.** Layout of PV modules.

A geometric analysis yielding the following equation between adjacent PV modules is presented as follows:

$$L_S = H \cdot \cot\alpha = H \cdot \cot(90 - |\phi - \delta|) \quad (6)$$

Different tilt angles have different spaces ($L_S$), affecting the installation of all PV modules and the detailed relationship behind this is described as follows.

$$A_{PV} = N \times L \times W \quad (7)$$

where $N$, $L$, and $W$ denote the total number of PV modules, the length of one PV panel and the width of one PV panel, respectively.

Table 1 presents the PV data that are used in this work [32].

**Table 1.** PV data.

| Items | Parameters | Items | Parameters |
|---|---|---|---|
| Life Time | 25 years | Efficiency | 14.5% |
| Cost of Investment | $1800/kW | Length of PV Panel | 1.47 m |
| Cost of Replacement | $1800/kW | Width of PV Panel | 0.68 m |
| Cost of Brackets | $1100/kW | Cost of Inverter | $655/kW |

2.2.2. Battery

Owing to the uncertainties of solar energy [33], a lead-acid battery is utilized as the ESS to regulate power fluctuations, taking the state of charge (SOC) into account. In this paper, the lead-acid battery plays a significant role in balancing fluctuations that are caused by the PV system. With the help of the battery, the PV generation system, together with the ESS, maintains a stable output power.

When the total power generated PV modules exceeds the desired output of the PV generation system, the battery bank is charged. The charging energy of the ESS at time t is obtained as follows:

$$E_{\mathrm{ESS}(t)} = E_{\mathrm{ESS}(t-1)} + \Delta P \cdot h \cdot \eta_{\mathrm{ch}} \tag{8}$$

where $E_{\mathrm{ESS}(s,t)}$ and $E_{\mathrm{ESS}(s,t-1)}$ are the charging energy of the ESS at times $t$ and $t$ – 1; $\Delta P$ is the difference between the expected power and the real output power of the PV system; and $\eta_{\mathrm{ch}}$ is the charging efficiency of the battery bank.

On the other hand, when the solar irradiation is insufficient and the power from the PV system is less than the expected value, then the battery bank is discharged, as described by Equation (9).

$$E_{ESS(t)} = E_{ESS(t-1)} - \Delta P \cdot h / \eta_{\mathrm{dis}} \tag{9}$$

Table 2 presents the specifications of the lead-acid battery [34].

**Table 2.** Battery data (lead-acid battery).

| Item | Parameters |
|---|---|
| Life Time | 8 years |
| Charge Efficiency | 75% |
| Discharge Efficiency | 100% |
| Cost of Investment | $100/kWh |
| Cost of Replacement | $100/kWh |

2.2.3. Diesel Generator

As the main power source in a hybrid ship power system, a diesel generator meets the load demand if the total power generated by both the PV modules and the ESS is too low. The fuel consumption of the diesel generator, $F_{\mathrm{d}}$ (L/h), depends on the output power and is defined as [35].

$$F_{\mathrm{d}} = a \cdot P_{\mathrm{d}} + b \cdot P_{\mathrm{dN}} \tag{10}$$

where $P_{\mathrm{d}}$ is the output power of the diesel generator; $P_{\mathrm{dN}}$ is the rated power; and $a$ = 0.246 (L/kwh) and $b$ = 0.0845 (L/kwh) are the coefficients of the consumption curve.

Different from a diesel generation on land, the diesel generator on a ship must ensure 100% reliability regardless of the use of renewable energy. Hence, the total capacity of the diesel generator in this oil tanker is 2 MW, which is enough to supply the maximum load.

#### 2.2.4. Load

The characteristics of the load profile are critical in planning a reliable hybrid ship power system. The load condition is changing with the different operating situations of the ship. Figure 4 plots the total load of the oil tanker in five operating situations, which are detailed in Table 3. Specifically, the five load conditions are 1580, 1790, 1650, 1290 and 500 kW corresponding to regular cruising, full-speed sailing, docking, loading/unloading and anchoring, respectively. The peak load is 1790 kW, reached when the ship is at full speed. The ship stops in six cities, Dalian (China), Shanghai (China), Hong Kong (China), Singapore, Matara (Sri Lanka), and Aden (Yemen), for trading and maintenance. When the ship is sailing on the ocean, it is always at full speed; when it sails in the Strait of Malacca, it is in its regular cruising mode.

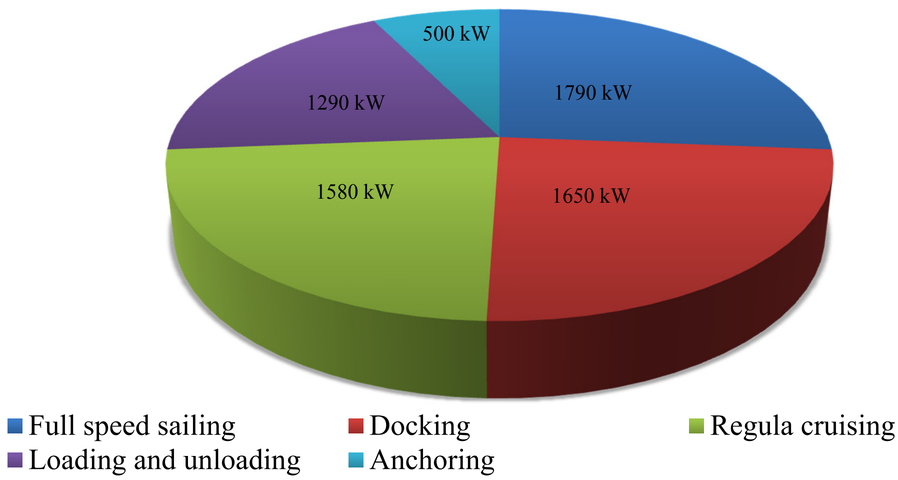


**Figure 4.** Five load conditions.

**Table 3.** Duration associated with each load condition.

| Operating Mode | Dalian in China | Shanghai in China | Hong Kong in China | Singapore | Matara in Sri Lanka | Aden in Yemen |
|---|---|---|---|---|---|---|
| Docking | 2 h | 2 h | 2 h | 2 h | 2 h | 2 h |
| Loading and unloading | 6 h | 8 h | 14 h | 12 h | 7 h | 6 h |
| Anchoring | 4 h | 0 h | 4 h | 5 h | 6 h | 4 h |

## 3. Problem Formulation

### *3.1. Objective Function*

This work proposes a novel method for optimizing the size of the ESS that accounts for the difference between the expected value and actual output power of a PV system. The goal of the studied problem is to minimize the investment and waste power costs of the ship's power system and the emissions from the diesel generators, while satisfying the operational constraints. The multi-objective functions are as follows:

$$\min\begin{cases} f_1 = (C^{\text{ESS}}_{\text{capital}} + C^{\text{ESS}}_{\text{replacement}})\cdot C_{\text{ESS}} + \text{CRF}\cdot(Price\cdot F_1 + Price\cdot F_2) \\ f_2 = N\sum_{t=1}^{N} Em_{\text{CO}_2}\cdot(aP_{\text{d}} + bP_{\text{dN}}) \end{cases} \tag{11}$$

The first objective function in Equation (11) is to calculate the total cost of the hybrid ship power system by optimally allocating ESS and determining the outputs of diesel generator under consideration of the change of the solar irradiation and shiploads. Due to the environmental concern, the emission in the second objective function of Equation (11) is to reduce the gaseous pollutants.

More specifically, the total cost consists of the investment cost of the ESS and the wasted power cost of the PV system, specified as net present values. The wasted power cost is defined as follows:

$$\begin{cases} F_1 = N\sum_{t=1}^{T} S_1(t)[P_{\text{ESS}(t)}\Delta t - (C_{\text{ESSmax}} - C_{\text{ESS}}(t-1))] + N\sum_{t=1}^{T} S_2(t)(\Delta P\Delta t - P_{\text{ESSmax}}\Delta t) \\ F_2 = N\sum_{t=1}^{T} S_3(t)[|P_{\text{ESS}}\Delta t| - (C_{\text{ESS}}(t-1) - C_{\text{ESSmin}})] + N\sum_{t=1}^{T} S_4(t)(\Delta P\Delta t - P_{\text{ESSmax}}\Delta t) \end{cases} \tag{12}$$

where $S_1(t)$, $S_2(t)$, , $S_3(t)$, and $S_4(t)$ denote Boolean variables that take the value 0 or 1, based on the ship's operating situation; $Price$ is the price for wasted power that is generated by the PV system; $C^{\text{ESS}}_{\text{capital}}$ and $C^{\text{ESS}}_{\text{replacement}}$ denote the costs of installation and replacement for the lead-acid battery; $C_{\text{ESS}}$ is the capacity of the ESS (kWh); and $\Delta P$ is the difference between the expected and real output power of the PV system.

It should be noted that a larger capacity of ESS ($C_{\text{ESS}}$) will reduce the wasted power of PV system ($F_1$ and $F_2$) but increase the capital and replacement fee for ESS. As a consequence, an optimal capacity of ESS is necessary in a hybrid ship power system.

To convert the initial cost into an annual capital cost, the capital recovery factor (CRF), given by Equation (13) is used:

$$\text{CRF} = \frac{r(1+r)^y}{(1+r)^y - 1} \tag{13}$$

where $r$ is the interest rate and y denotes the life span of the PV system or the ESS.

### *3.2. Constraints*

A hybrid PV/diesel/ESS ship power system must satisfy the following operational constraints:

$$P_{\text{d min}} \le P_{\text{d}(\text{s},t)} \le P_{\text{d max}} \tag{14}$$

$$C_{\text{ESSmin}} \le C_{\text{ESS}} \le C_{\text{ESSmax}} \tag{15}$$

$$-P_{\text{ESSmax}} \le P_{\text{ESS}}(t) < P_{\text{ESSmax}} \tag{16}$$

where $P_{\text{d}(t)}$, $P_{\text{PV}(t)}$, and $E_{\text{ESS}(t)}$ represent the outputs of the diesel generator, the PV system and ESS, respectively, at time $t$.

The diesel generator can supply all of the power for the total load so ESS does not have to ensure the 100% stability to balance the fluctuations caused by PV system. Accordingly, the power fluctuation within a 95% confidence interval is considered herein such that when the output power of the PV system fluctuates, the probability that the ESS guarantee the stability is 95%. In Equation (17) provides the related constraint.

$$P_{\mathrm{r}}\left\{\Delta P(i) \le \Delta P_{\max}\right\} \ge \beta \tag{17}$$

The active power should be balanced at time t as follows:

$$P_{\mathrm{d}(t)} + P_{\mathrm{PV}(t)} + P_{\mathrm{ESS}(t)} = P_{\mathrm{Load}(t)} \tag{18}$$

where $P_{\mathrm{Load}(t)}$ is the load demand at time *t*.

## 4. Solution Method

Due to the complexity and nonlinearity of the optimal sizing problem, the Multi-Objective Genetic Algorithm (MOGA) is utilized in this paper to find the best allocation for the ESS.

The Genetic Algorithm (GA) for solving the constrained nonlinear optimization problem is based on natural selection [36]. Generally, a GA uses three operators (selection, crossover and mutation) to imitate the process of natural evolution. The GA begins with a random population of individuals (called chromosomes). Herein, it is initialized using the diesel generators' output power for 4800 h, and the capacity of the battery. Each chromosome represents a solution to the optimization problem and the population is evaluated by the fitness function. If the chromosome has a lower cost and emission of hybrid ship system than the lowest value obtained at the previous iterations, this system configuration (chromosome) is considered to be the optimal solution to the minimization problem in this iteration. This optimal solution will be replaced by better solutions, if any, that are produced subsequently during the program evolution. After the selection process, the optimal solution will then be subjected to crossover and mutation operations in order to produce the next generation population until a pre-specified number of generations have been reached or when a criterion that determines the convergence is satisfied. The flowchart in Figure 5 illustrates the proposed MOGA methodology.

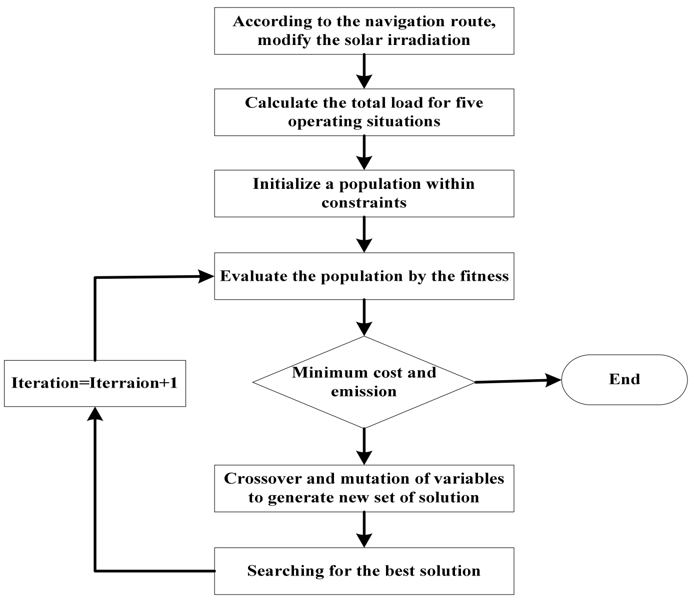


**Figure 5.** Flowchart of proposed method.

## 5. Simulation Result and Discussion

### *5.1. Optimal Tilt Angle of PV Arrays*

Owing to the significant effect of the tilt angle on the output of a PV system, various ways to install PV arrays with respect to parameters in Equations (1)–(8) are examined, taking into account the shading factor. Figure 6 shows the different ways to locating PV systems on ship.

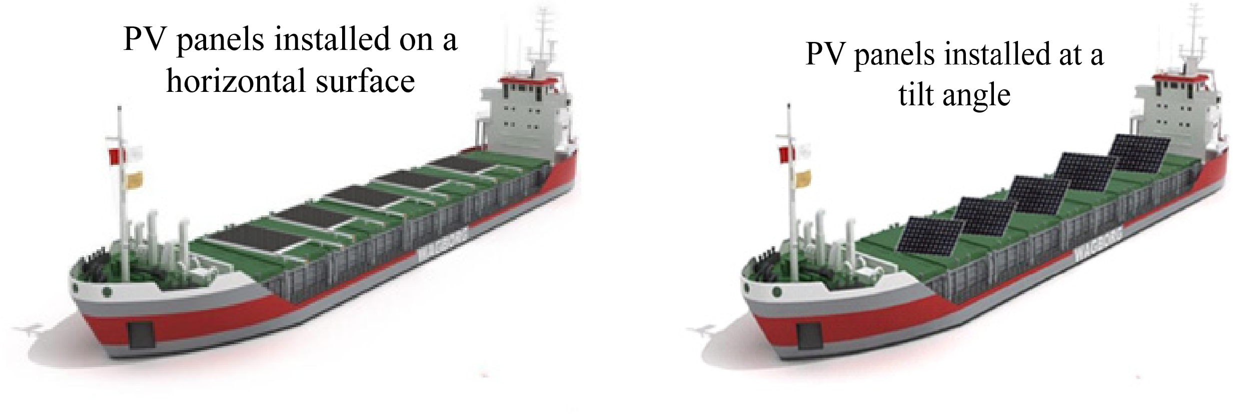


**Figure 6.** Different PV panel installation patterns.

The solar irradiation is sampled hourly along the route from Dalian in China to Aden in Yemen. Based on data from the GeoModel Solar Company [37], the hourly solar irradiation is modified using the method that was discussed in Section 2, yielding data that are presented in Figure 7.

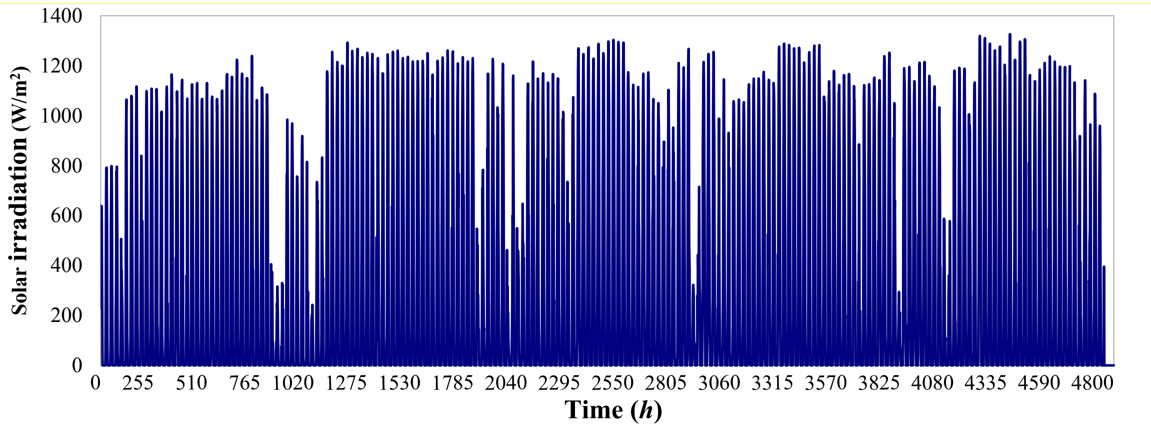


**Figure 7.** Solar irradiation along the ship's route.

Based on the above solar irradiation, the amount of the power that is generated by PV system at different angles over 25 years is calculated and the shading factor is taken into consideration, as shown in Figure 8.

Figure 8 reveals that the PV system generates the most amount of power, 350,159 kWh, when it is installed on a horizontal surface. Moreover, the power produced by PV modules decreases as the tilt angle increases. When the PV modules at 45°, the PV system produced the least power (142,536 kWh), 59.29% less than when the system was installed horizontally.


**Figure 8.** Total power generated by PV system over 25 years.

Figure 9 presents the profit that is gained over 25 years by installing PV arrays at various angles. As seen in Figure 9, installing a PV system on a horizontal surface maximizes profit at $1,381,952. Installing the PV system at a tilt angle reduces profit; the lowest profit is $354,525, which is $1,027,427 less than that achieved when the system is installed horizontally.

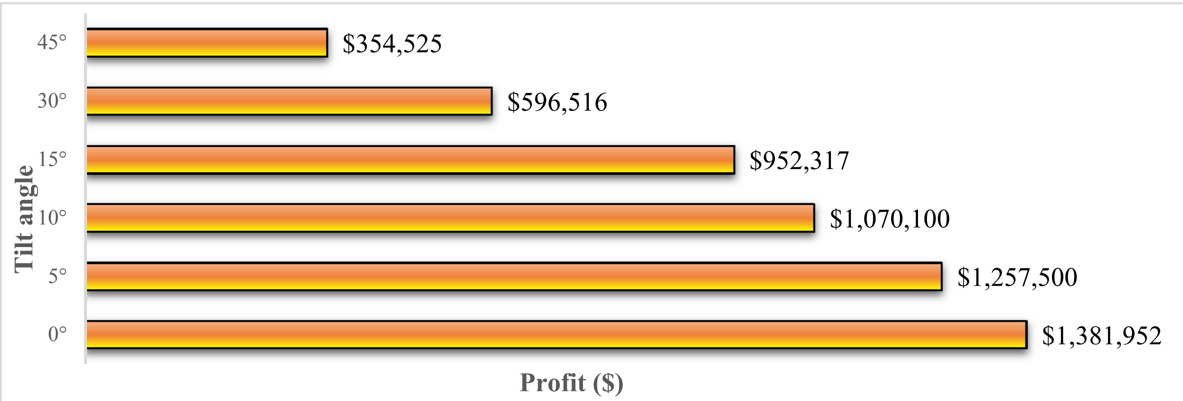


**Figure 9.** Profit generated by PV system over 25 years.

Consequently, given the solar irradiation along the route, the PV system should be installed on a horizontal surface to enable the ship to exploit the solar energy effectively.

### *5.2. Economic Analysis*

This work developed a novel method that utilized the difference between the expected and real output power of PV system to optimize the size of the ESS on ship; Figure 10 plots this difference. The expected output power by the PV system is 218 kW, as the solar irradiation changes, the combination of the ESS with the diesel generator smooths the variations in the power output.

Three cases are studied to demonstrate the effectiveness of the proposed MOGA method and the effects of the integration of solar power into a ship's power system, under various loading conditions, taking into account the ESSs that are also used.

Case 1: Cost analysis of diesel generator only;
Case 2: Cost analysis of diesel generator and PV array only;
Case 3: Multi-objective optimization, considering costs of diesel generator, PV, ESS and $CO_2$ emissions.

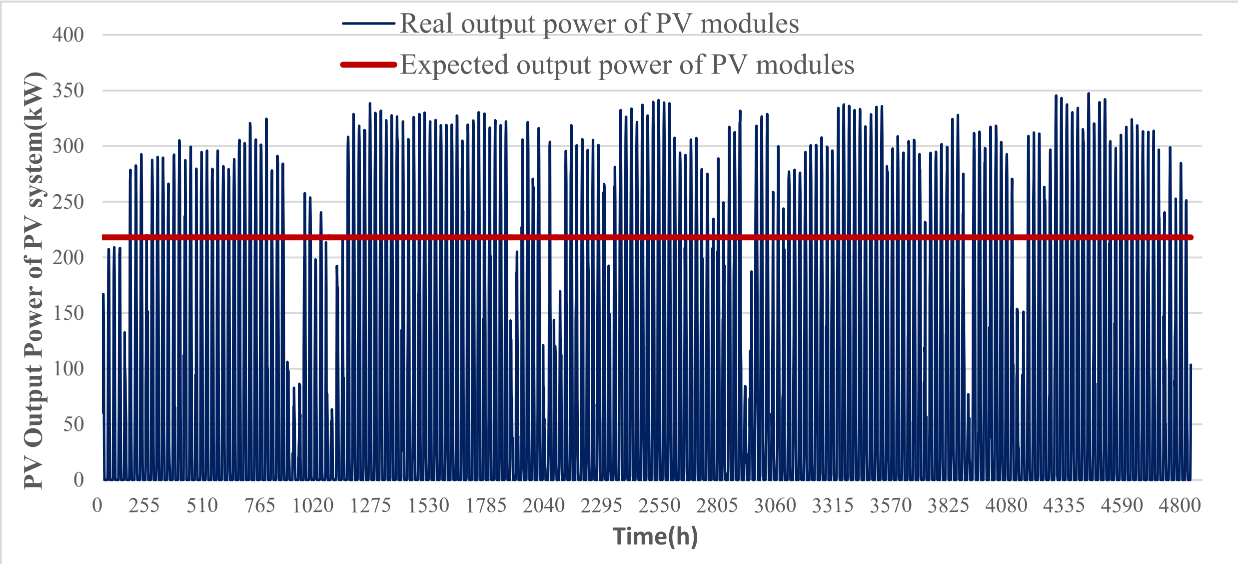


**Figure 10.** Expected and real output power by PV system.

Table 4 presents the total costs and emissions of the ship system associated with the output of the diesel generator in Case 1, Case 2, and Case 3.

**Table 4.** Net present cost and emission with total diesel output.

| Item | Case 1 | Case 2 | Case 3 |
|---|---|---|---|
| PV size (kW) | 0 | 292 | 292 |
| ESS size (kW) | 0 | 0 | 140 |
| ESS capacity (kWh) | 0 | 0 | 110 |
| PV installation cost ($) | 0 | 522,000 | 522,000 |
| PV replacement cost ($) | 0 | 522,000 | 522,000 |
| ESS installation cost ($) | 0 | 0 | 583,975 |
| ESS replacement cost ($) | 0 | 0 | 583,975 |
| Total NPC ($) | 2,320,645 | 1,258,245 | 1,105,975 |
| Emission (kg) | 55,314,000 | 49,557,769 | 29,853,731 |
| Total diesel output (kWh) | 8,720,000 | 2,766,500 | 2,070,326 |

Table 4 indicates that (a) solar energy and a battery both reduce the total diesel output power; (b) the emissions are reduced from 55,314,000 kg in Case 1 to 29,853,731 kg in Case 3. In Case 1, the total load demand is supplied only by the diesel generators, so the cost is the highest, being $2,320,645, and the problem of emissions is the most serious. Even though the ship's power system includes PV generation, Case 2 is associated with a high system cost ($ 1,258,245), implying that the ESS is required in ship power system and optimization method must be performed. It should be noted that the use of a lead-acid battery and the MOGA algorithm in Case 3 reduces the system cost and the total emission to their lowest value. More specifically, the total cost of hybrid ship power system in Case 3 is $ 1,105,975 associated with 29,853,731 kg of emissions, which is less than the half of that in Case 1. Compared to Case 2, the total cost is reduced by 12.1%. Suppose that the life span of the hybrid ship power system is 25 years; then $ 3,806,750 is saved. This result demonstrates that the size of the lead-acid battery selected by the proposed MOGA algorithm is much better than in the other cases.

In addition, after the allocation of ESS was optimized, the cooperation of various types of distributed generations to supply the power for the shipload was analyzed. The simulation result demonstrates the importance of the ESS in the hybrid ship power system and Figure 11 shows the output power of various generation systems when the solar irradiation is changing the most during the ship sailing.

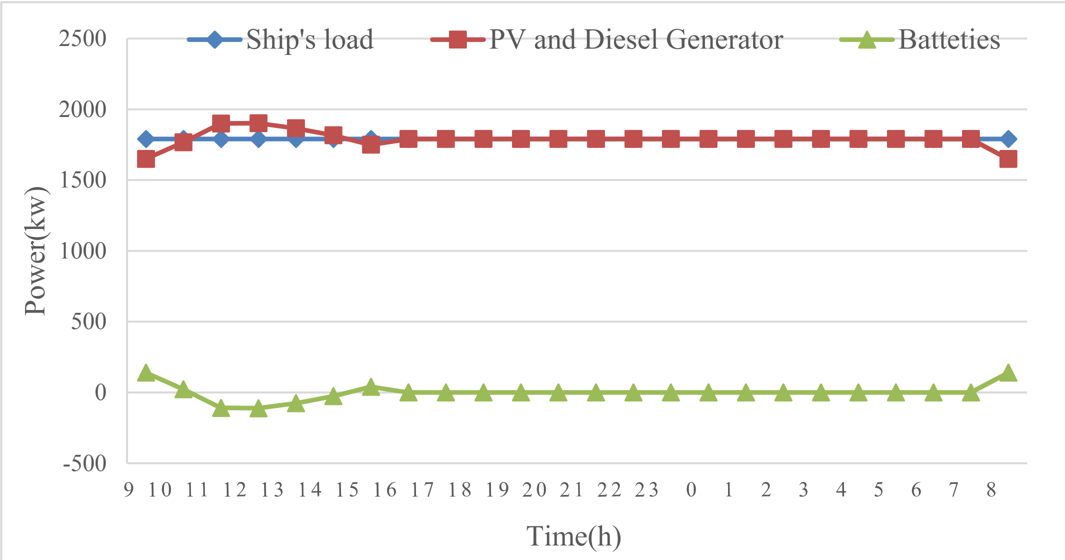


**Figure 11.** Load and outputs of diesel generator, PV modules, and ESS.

## 6. Conclusions

In this paper, the layout of PV arrays in ship power system is optimized. A novel methodology is proposed for determining the optimal size of the ESS and output of diesel generator in a hybrid PV/diesel/ESS power system on ship. Hourly irradiation is modeled under consideration of the date, time, longitude, latitude and other factors along the route from Dalian in China to Aden in Yemen. Furthermore, hourly loads are modeled under five operating conditions, the MOGA algorithm is used to search the optimal solution for the sizing optimization and emission problems. The simulation results show that (i) the PV panels on the shipboard should be installed horizontally; (ii) the profit generated by the PV system on shipboard decreases with the increase of the tilt angle; and (iii) with the help of an optimal allocation of ESS, the net present costs and emissions of the hybrid PV/diesel/ESS ship system can be minimized.

## Acknowledgments

This study was financially supported by the Ministry of Industry and Information Technology in cooperation with the Ministry of Finance under grant GK110900004 and by fundamental research funds for the central universities under HEUCFX41401.

## Author Contributions

All authors contributed to this collaborative work. Hai Lan and Jinfeng Dai performed the research and discussed the results. Shuli Wen, Ying-Yi Hong, David C. Yu and Yifei Bai suggested the research idea and contributed to the writing and revision of the paper. All authors approved the manuscript.

## Conflicts of Interest

The authors declare no conflict of interest.

## References

1. The International Convention for the Prevention of Pollution from Ships. Available online: http://www.eisil.org/index.php?t=link_details&id=609&cat=424 (accessed on 19 May 2005).
2. Zahedi, B.; Norum, L.E.; Ludvigsen, K.B. Optimized efficiency of all-electric ships by dc hybrid power systems. *J. Power Source* **2014**, *255*, 341–354.
3. Bocca, A.; Chiavazzo, E.; Macii, A.; Asinari, P. Solar energy potential assessment: An overview and a fast modeling approach with application to Italy. *Renew. Sustain. Energy Rev*. **2015**, *49*, 291–296.
4. Najafi, G.; Ghobadian, B.; Mamat, R.; Yusaf, T.; Azmi, W.H. Solar energy in Iran: Current state and outlook. *Renew. Sustain. Energy Rev*. **2015**, *49*, 931–942.
5. Balcombe, P.; Rigby, D.; Azapagic, A. Environmental impacts of microgeneration: Integrating solar PV, Stirling engine CHP and battery storage. *Appl. Energy* **2015**, *139*, 245–259.
6. Curry, N.; Pillay, P. Integrating solar energy into an urban small-scale anaerobic digester for improved performance. *Renew. Energy* **2015**, *83*, 280–293.
7. Freitas, S.; Serra, F.; Brito, M.C. PV layout optimization: String tiling using a multi-objective genetic algorithm. *Sol. Energy* **2015**, *118*, 562–574.
8. Martinez-Rubio, A.; Sanz-Adan, F.; Santamaria, J. Optimal design of photovoltaic energy collectors with mutual shading for pre-existing building roofs. *Renew. Energy* **2015**, *78*, 666–678.
9. Mohammadi, S.; de Vries, B.; Schaefer, W. Modeling the allocation and economic evaluation of PV panels and wind turbines in urban areas. *Procedia Environ. Sci*. **2014**, *22*, 333–351.
10. Dolara, A.; Lazaroiu, G.C.; Leva, S.; Manzolini, G. Experimental investigation of partial shading scenarios on PV (photovoltaic) modules. *Energy* **2013**, *55*, 466–475.
11. Sarmah, N.; Mallick, T.K. Design, fabrication and outdoor performance analysis of a low concentrating photovoltaic system. *Sol. Energy* **2015**, *112*, 361–372.
12. Richardson, D.B.; Harvey, L.D.D. Strategies for correlating solar PV array production with electricity demand. *Renew. Energy* **2015**, *76*, 432–440.
13. Karakose, M.; Baygin, M. An Analysis Approach for optimization based reconfiguration in photovoltaic arrays. In Proceedings of the IEEE 23th International Symposium on Industrial Electronics, Istanbul, Turkey, 1–4 June 2014; pp. 954–959.
14. Sharma, P.; Duttagupta, S.P.; Agarwal, V. A novel and universal model for accurate prediction of PV module characteristics for power optimization under various design layouts and dynamic environmental conditions. In Proceedings of the IEEE International Conference on Power Electronics, Drives and Energy Systems, Bengaluru, India, 16–19 December 2012; pp. 1–6.

15. Midtgard, O.-M.; Sætre, T.O.; Yordanov, G.; Imenes, A.G.; Nge, C.L. A qualitative examination of performance and energy yield of photovoltaic modules in southern Norway. *Renew. Energy* **2010**, *35*, 1266–1274.
16. Shirzadi, S.; Hizam, H.; Wahab, N.I.A. Mismatch losses minimization in photovoltaic arrays by arranging modules applying a genetic algorithm. *Sol. Energy* **2014**, *108*, 467–478.
17. Díaz-Dorado, E.; Suárez-García, A.; Carrillo, C.J.; Cidrás, J. Optimal distribution for photovoltaic solar trackers to minimize power losses caused by shadows. *Renew. Energy* **2011**, *36*, 1826–1835.
18. Rani, B.I.; Ilango, G.S.; Nagamani, C. Enhanced power generation from PV array under partial shading conditions by shade dispersion using Su Do Ku configuration. *IEEE Trans. Sustain. Energy* **2013**, *4*, 594–601.
19. Paraskevadaki, E.V.; Papathanassiou, S.A. Evaluation of MPP voltage and power of mc-Si PV modules in partial shading conditions. *IEEE Trans. Energy Convers*. **2011**, *26*, 923–932.
20. Zhao, P.; Wang, J.; Dai, Y. Capacity allocation of a hybrid energy storage system for power system peak shaving at high wind power penetration level. *Renew. Energy* **2015**, *75*, 541–549.
21. Bianchi, M.; Branchini, L.; Ferrari, C.; Melino, F. Optimal sizing of grid-independent hybrid photovoltaic-battery power systems for household sector. *Appl. Energy* **2013**, *136*, 805–816.
22. Maleki, A.; Pourfayaz, F. Optimal sizing of autonomous hybrid photovoltaic/wind/battery power system with LPSP technology by using evolutionary algorithms. *Sol. Energy* **2015**, *115*, 471–483.
23. Aghamohammadi, M.R.; Abdolahinia, H. A new approach for optimal sizing of battery energy storage system for primary frequency control of islanded microgrid. *Int. J. Electr. Power Energy Syst*. **2014**, *54*, 325–333.
24. Bahmani-Firouzi, B.; Azizipanah-Abarghooee, R. Optimal sizing of battery energy storage for micro-grid operation management using a new improved bat algorithm. *Int. J. Electr. Power Energy Syst*. **2014**, *56*, 42–54.
25. Fossati, J.P.; Galarza, A.; Martín-villate, A.; Font, L. A method for optimal sizing energy storage systems for microgrids. *Renew. Energy*. **2015**, *77*, 539–549.
26. Chen, C.; Duan, S.; Cai, T.; Liu, B.; Hu, G. Optimal allocation and economic analysis of energy storage system in microgrids. *IEEE Trans. Power Electron*. **2011**, *26*, 2762–2773.
27. Ovrum, E.; Bergh, T.F. Modelling lithium-ion battery hybrid ship crane operation. *Appl. Energy* **2015**, *152*, 162–172.
28. Dedes, E.K.; Hudson, D.A.; Turnock, S.R. Assessing the potential of hybrid energy technology to reduce exhaust emissions from global shipping. *Energy Policy* **2012**, *40*, 204–218.
29. Andrews, R.W.; Pearce, J.M. The effect of spectral albedo on amorphous silicon and crystalline silicon solar photovoltaic device performance. *Sol. Energy* **2013**, *91*, 233–241.
30. Da-Rosa, A.V. *Fundamentals of Renewable Energy Processes*, 2nd ed.; Elsevier Academic Press: Waltham, MA, USA, 2009.
31. Melo, E.G.; Almeida, M.P.; Zilles, R.; Grimoni, J.A.B. Using a shading matrix to estimate the shading factor and the irradiation in a three-dimensional model of a receiving surface in an urban environment. *Sol. Energy* **2013**, *92*, 15–25.
32. Feldman, D.; Barbose, G.; Margolis, R.; Darghouth, N.; James, T.; Weaver, S.; Goodrich, A.; Wiser, R. Photovoltaic System Pricing Trends: Historical, Recent, and Near-Term Projections 2014 Edition. Available online: http://eetd.lbl.gov/sites/all/files/presentation1.pdf (accessed on 22 September 2014).

33. El Fathi, A.; Nkhaili, L.; Bennouna, A.; Outzourhit, A. Performance parameters of a standalone PV plant. *Energy Convers. Manag*. **2014**, *86*, 490–495.
34. Dufo-López, R.; Lujano-Rojas, J.M.; Bernal-Agustín, J.L. Comparison of different lead-acid battery lifetime prediction models for use in simulation of stand-alone photovoltaic systems. *Appl. Energy* **2014**, *115*, 242–253.
35. Maleki, A.; Pourfayaz, F. Sizing of stand-alone photovoltaic/wind/diesel system with battery and fuel cell storage devices by harmony search algorithm. *J. Energy Storage* **2015**, *2*, 30–42.
36. Yang, H.; Zhou, W.; Lu, L.; Fang, Z. Optimal sizing method for stand-alone hybrid solar-wind system with LPSP technology by using genetic algorithm. *Sol. Energy* **2008**, *82*, 354–367.
37. Geomodel Solar Company. Solar and PV Data. Available online: http://solargis.info/doc/solar-and-pv-data (accessed on 20 March 2014).